Journal of Materials and Electronic Devices 4 (2020) 14-20

JOURNAL OF MATERIALS AND ELECTRONIC DEVICES
FYTRONIX JMED http://dergi-fytronix.com/

On the temperature dependent reverse current conduction mechanisms in (AuZn)/TiO_2/p-GaAs MIS structures

Yasemin ŞAFAK ASAR

Department of Physcis, Faculty of Science, Gazi University 06500 Ankara/Turkey

In this study, reverse bias current conductance mechanisms of (AuZn)/TiO_2/p-GaAs metal-insulator-semiconductor (MIS) structures were investigated in the temperature range of 80-290 K. In this temperature range, the leakage current was dominated by Schottky emission and Fowler-Nordheim tunneling in the low and moderate field region, respectively. The analysis of the reverse current-voltage characteristics underlines that the main process in leakage current flow is the carrier injection through a barrier at the material electrode interface.

Keywords: Titanium dioxide; Fowler Nordheim tunneling, Poole-Frenkel emission, Schottky emission,.

Submission Date: 06 May 2020
Acceptance Date: 04 June 2020

Corresponding author: yaseminsafak@gazi.edu.tr

1. Introduction

Gallium arsenide (GaAs) is one of the most popular semiconductors for high-speed and low-power applications because of having a direct energy band gap, high electron mobility, high breakdown voltage, mechanical stability and lower power dissipation [1-4]. Therefore, GaAs-based structures are widely used as an essential part of the high speed microelectronics and optoelectronic applications in different fields of technology [5-9]. Nevertheless, the requirement of good quality interfacial insulator layer and the existence of Fermi level pinning, due to localized electronic states introduced by defects and impurities [10,11], has deteriorated their use in microelectronic industry. This undesired condition can be impeded by inserting an insulator layer between metal and semiconductor. Therefore, a metal-semiconductor (MS) structure turns into metal-insulator/oxide-semiconductor (MIS/MOS) structure. Such an interfacial insulator layer native or deposited have a strong influence on the performance and conduction mechanisms of these devices. When thickness of insulator layer is less than 30 Å, charges at surface states or traps correlates with metal, whereas they correlate with semiconductor if insulator layer thickness is larger than 30 Å [12]. In addition, when insulator layer thickness is sufficiently large enough (≥500 Å), MIS structure acts as a MOS capacitor, rather than a MIS type structure. The continual decrease in silicon transistors has compelled gate oxides to thickness below 50 Å. At these dimensions leakage current, which prevents the device performance, is increased by direct tunneling [13]. The presence of direct tunneling through the insulator layers has led to many studies on alternative oxides with high dielectric constant. Also, active dangling bonds on the semiconductor surface cannot be passivated by the insulator layer formed with the known techniques of oxidation or deposition. Otherwise, the use of such a high dielectric material can decrease the amount of dangling bonds and also the leakage current. A number of high-k materials such as TiO_2, HfO_2 and Al_2O_3 [14] are studied in GaAs based devices nowadays. Among these dielectric materials, TiO_2 can be evaluated as more promising nominee with its extraordinary high dielectric constant. Bulk TiO_2 is known to occur one of three different polycrystalline structures: anatase, rutile and brookite. Among them, brookite is unstable. The anatase phase is composed in thin films at temperatures under 600 ^oC and bulk anatase TiO_2 has a dielectric constant to be 48 [13,15]. The transformation to the rutile phase occurs around 800 ^oC. Rutile is the most stable phase and generally preferred for optical applications because of its higher refractive index [16]. Anatase is metastable at room temperature and is used in many kind of applications including photo-catalysis [17], gas sensing [18,19] and solar energy conversion [20,21].

There are several methods to form TiO_2 layer such as traditional thermal oxidation, anodic oxidation, sol-gel, electro-spining and sputtering. Among them sputtering method can be suitable for growing high quality films, high density, high adhesion and high hardness with good uniformity of the film thickness at low substrate temperatures [1,2,22]. The reverse bias current conduction mechanisms in thin films can be classified into two groups: interfaced-controlled and bulk-controlled mechanisms. Carrier injection through a barrier at the material electrode interface Schottky emission (SE) and Fowler-Nordheim (FN) tunneling belong the first group. The second group includes several mechanisms such as Poole-Frenkel emission (PFE) and space charge limited conduction [23-25].

In this study, we aimed to clarify the conduction mechanism of the leakage current in (AuZn)/TiO2/p-GaAs MIS structures in the temperature range of 80-290 K.

2.-Experimental Details

(AuZn)/TiO_2/p-GaAs(110) MIS structures were fabricated to investigate the reverse bias current conduction mechanisms through the insulator/oxide layer. First, the Ti/Au alloy ohmic contact was formed by deposition of high purity (99.999%) Ti (300 Å) and Au (1900 Å) at 400 ˚C and then the sample was annealed 370 ˚C to achieve good ohmic contact behavior. After this, TiO_2 thin film with 400 Å thickness was deposited on the sample at 200 ˚C. High purity Ti target and specific Ar+O_2 reactive gas mixture (Ar/O_2=80/20 sccm) was used to form TiO_2 thin film. The thickness of the TiO_2 thin film was confirmed by stylus type profilometer. After, the 2 mm dot shaped AuZn rectifier contacts with 1000 Å thickness were evaporated onto TiO_2 thin film at room temperature. The structural properties and the interface characteristics of the sample were analyzed by means of X-ray diffraction (XRD), atomic force microscopy (AFM) and secondary ion mass spectrometry (SIMS) measurements. More information about the feature of the deposition parameter and the characterization of the sample can be found in our previous study [1].

The reverse bias current-voltage measurements were performed by using a Keithly 2400 source meter in the temperature range of 140-290 K by the step of 30 K in a temperature-controlled Janis vpf-474/5 cryostat, which enable us to measure in the temperature range of 77-450 K. The sample temperature was always monitored by using a Lake Shore model 321 auto-tuning temperature controllers with sensitivity better than ±0.1 K. all measurements were carried out with the help of a microcomputer through an IEEE-488 AC/DC converter card.

3.- Results and Discussion

The junction fabricated to form (AuZn)/TiO_2/p-GaAs(110) MIS structure exhibits rectifying behavior, as shown in Fig.1. In the reverse bias region, however, the current increases with increase of reverse applied bias voltage as seen in the semi-logarithmic $I - V$ plot of the structure. This clearly shows a discrepancy with the simple thermionic emission where for $V < -\frac{3kT}{q}$. The reverse bias current should saturate as described [23-26]:

$$I(V) = AA^{*}T^{2}\exp(-\frac{q\Phi_B}{kT}) \quad (1)$$

where A^* is the Richardson constant (=74.4 for p-GaAs), A is the diode area (=0.0314 cm^2), k is the Boltzmann constant, T is the temperature in K and Φ_B is the barrier height of the junction. The non-saturating current under reverse bias propounds that the barrier height is a function of bias voltage and temperature.

$$\Phi_B(V_i) = \frac{kT}{q}Ln(\frac{AA^{*}T^{2}}{I_i}) \quad (2)$$

Fig. 2 shows the voltage dependent barrier height values calculated from Eq. 2. in the temperature range of 140-290 K. The calculated values of Φ_B decrease with the increase of the reverse bias voltage for all temperatures. To explain the reduction of barrier height with the increase of reverse bias voltage, electric-field enhanced thermionic emission was studied by Schottky [23] and Poole-Frenkel [23] emission mechanisms.

Schottky Emission (SE)

The SE generated by the thermionic effect is induced by electron transport across the potential energy barrier at a metal/insulator interface. Generally, the Schottky conduction process is an electrode-limited conductivity that depends on the barrier between the metal and insulator layer and has the tendency to occur for the insulators with fewer defects. The current density associated with SE is given by [23-29]:

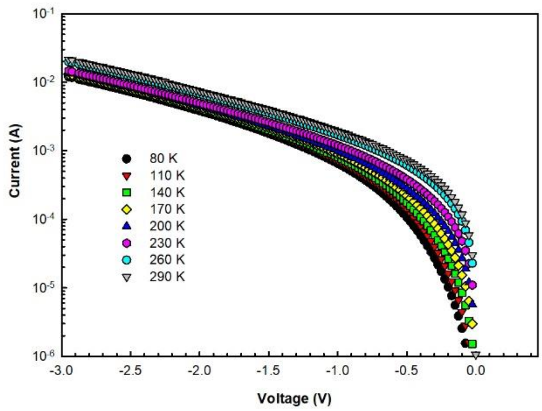

Figure 1. *The semi-logarithmic I-V plot of (AuZn)/TiO₂/p-GaAs(110) MIS structure in the temperature range of 140-290 K.*

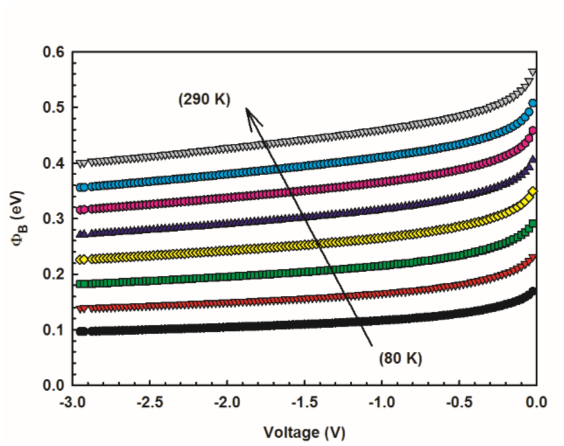

Figure 2. *The voltage dependent barrier height values in the temperature range of 80-290 K*

$$J_S = T^2 \exp\left[\frac{q}{kT}\sqrt{\frac{qE_b}{4\pi\varepsilon_0\varepsilon_i}}\right] \quad (3)$$

where E_b is the electric field in the semiconductor barrier at metal/semiconductor interface, ε_i is the dielectric constant of the insulator layer and ε_o is the permittivity of free space.

Schottky emission for the (AuZn)/TiO_2/p-GaAs MIS structure has been shown in terms of $\left(J/T^2\right)$ vs $E^{1/2}$ plot from the experimental $I-V$ data and given in Fig. 3 (a) and the linear behavior of the SE was given in Fig. 3 (b). It can be concluded from Fig. 3 (b) the straight-line characteristic at low electric field/voltage $(V = (-0.05)V - (-0.20)V)$ confirms the Schottky emission.

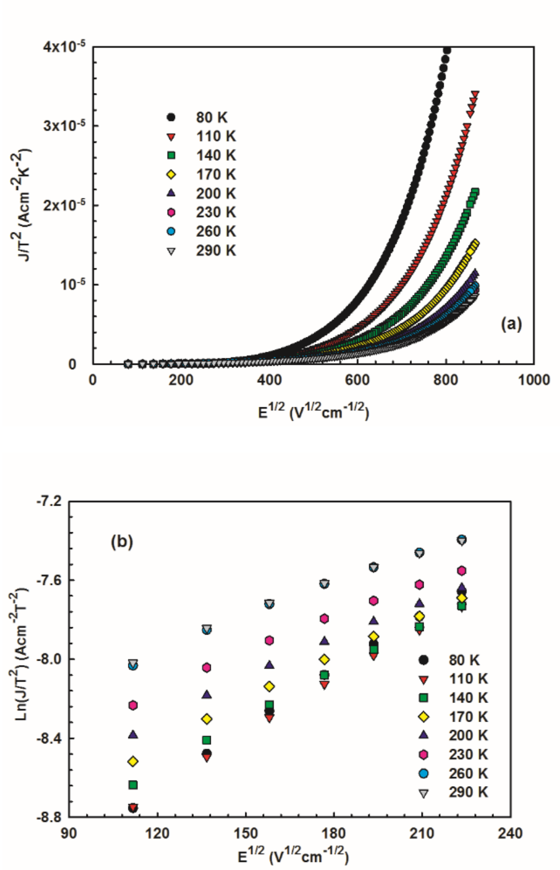

Figure 3. *(a) and (b) The Schottky Emission for the (AuZn)/TiO₂/p-GaAs MIS structure in terms*

Poole-Frenkel Emission (PFE)

Poole-Frenkel emission can be described as electric-field enhanced thermal emission from a trap state into a continuum of electronic states which can be usually found in the conduction band in an insulator. In other words; this is a thermally alleviated emission of charge carriers from Coulombic centers in the bulk of a dielectric or a semiconductor, enhanced by the application of an electric field. Emission of the electrons is checked by the electric filed, which is effective on the reduction of the barrier height on one side of the trap, thus give rise to the probability of the electron escaping from the trap. For this reason, the PFE is a bulk-limited conduction process which depends on the addition of the traps substantial in the bulk of the insulator layer. The current density associated with PFE is given by [26-34]:

$$J_{PF} = \text{Eexp}\left[\frac{q}{kT}\sqrt{\frac{qE}{\pi\varepsilon_0\varepsilon_i}}\right] \quad (4)$$

Poole-Frenkel emission for the (AuZn)/TiO_2/p-GaAs MIS structure has been shown in terms of $({}^{J}/_{E})$ vs $E^{1/2}$ plot from the experimental $I-V$ data and given in Fig. 4 (a). In Fig 4 (b), the linear behavior of the Poole-Frenkel emission, the straight-line characteristic at low electric field/voltage (at $V = (-0.15)V - (-0.45)V$) confirms the Poole-Frenkel emission.

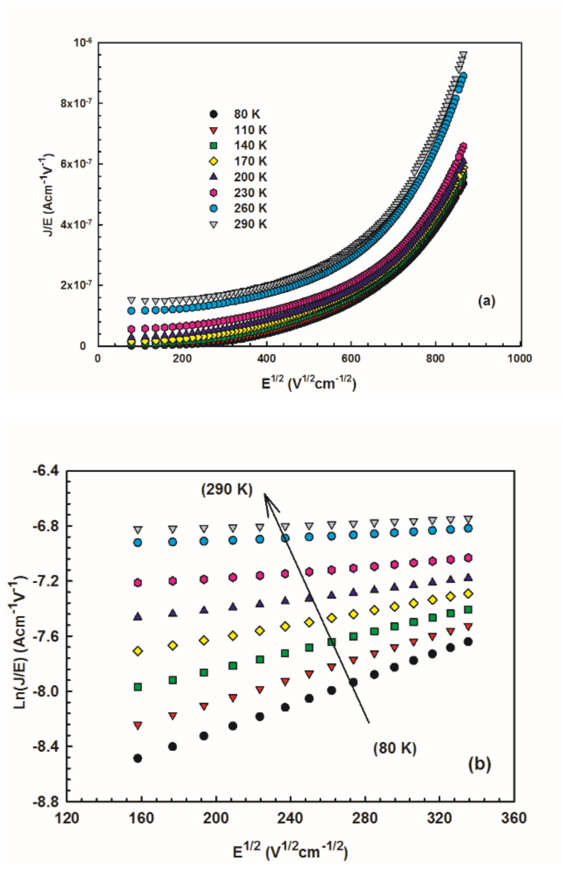

Figure 4. *(a) and (b) Measured reverse bias current density divided by electric field vs square root of electric field and the linear behavior of the Poole-Frenkel emission of (AuZn)/TiO_2/p-GaAs MIS structure at various temperatures.*

If the PFE dominates in the reverse current, then the plot of $Ln\left({}^{J}/_{E}\right)$ vs $E^{1/2}$ should be linear. Similarly, if a linear plot is found for $Ln({}^{J}/_{T^2})$ vs $E^{1/2}$ then the Schottky mechanism dominate in the reverse bias region. The value of field-lowering coefficient of SE (β_S) is always half of the value of PFE (β_{PF}) as follows:

$$\beta_S = \frac{\beta_{PF}}{2} = \left(\frac{q}{\pi\varepsilon_i\varepsilon_0}\right)^{1/2} \quad (5)$$

where ε_i, is the permittivity of insulator TiO_2 layer and is equal to 48 [13,15,35], and ε_0 is the permittivity of free space. The theoretical and experimentally determined values of these coefficients were given in Table 1.

Table 1: The theoretical and experimentally determined values of field-lowering coefficient of Poole-Frenkel and Schottky emission mechanisms.

	Experimental (from the slope)	Theoretical $(\boldsymbol{\varepsilon_i = 48\varepsilon_0})$
Poole-Frenkel Emission (β_{PF})	6.75x10^{-5}	1.10x10^{-4}
Schottky Emission(β_S)	6.39x10^{-5}	5.48x10^{-5}

The calculated values field-lowering coefficient for SE and PFE by taking $\varepsilon_i = 48\varepsilon_0$ and using Eq. 5 are given in Table 1. It can be concluded from these results that the SE is the dominant conduction mechanism in the investigated region of reverse bias region. The coefficient experimentally determined for the SE is more close to the theoretical value than the PFE. This result can also be seen from the determined values of the dielectric constant for TiO_2. This time by using the experimental values of field-lowering coefficient for SE and PFE dielectric constant of TiO_2 can be calculated with the help of Eq. 5. The determined values of ε_{TiO_2} is 32 and 126 for the SE and PFE, respectively. Among these values 32 is in good agreement with the available literature [13,15,35].

Fowler-Nordheim Tunneling (FW)

The conduction mechanisms mentioned above are a function of the dielectric constant while Fowler-Nordheim tunneling is not. In high-k dielectrics, trap related mechanisms are effective at low voltages and fields, while FN tunneling dominates at high voltages and fields [30-33].

$$J_{FN} = E_b^2 \exp\left[-\frac{b}{E}\right] \quad (6)$$

$$b = \frac{4\sqrt{2m^*}(q\emptyset_b)^{3/2}}{3qh} = 7.134 \times 10^{16}(m^*\emptyset_b^3)^{1/2} \qquad (7)$$

where $m^* = 0.3m_0$ [32] is the electron effective mass and $\emptyset_b$ is the barrier height. From Eq. 6, we can plot the $Ln(J_{FN}/E_b^2)$ as a function of $(1/E)$. The temperature dependent and the linear Fowler-Nordheim relation of reverse bias characteristics for (AuZn)/TiO_2/p-GaAs MIS structure in the high electric field/voltage $(V = (-2.40)V - (-2.92)\,V)$, corresponding to $E_b = (0.60 - 0.73)\,{cm}/{MV}$, given in Fig. 5 (a) and (b), respectively, approving that FN tunneling is the dominant leakage mechanism in this region of the bias voltage. The calculated values of barrier height from the slope of the $Ln(J_{FN}/E_b^2)$ versus $(1/E_b)$ for all the temperatures were given in Table 2.

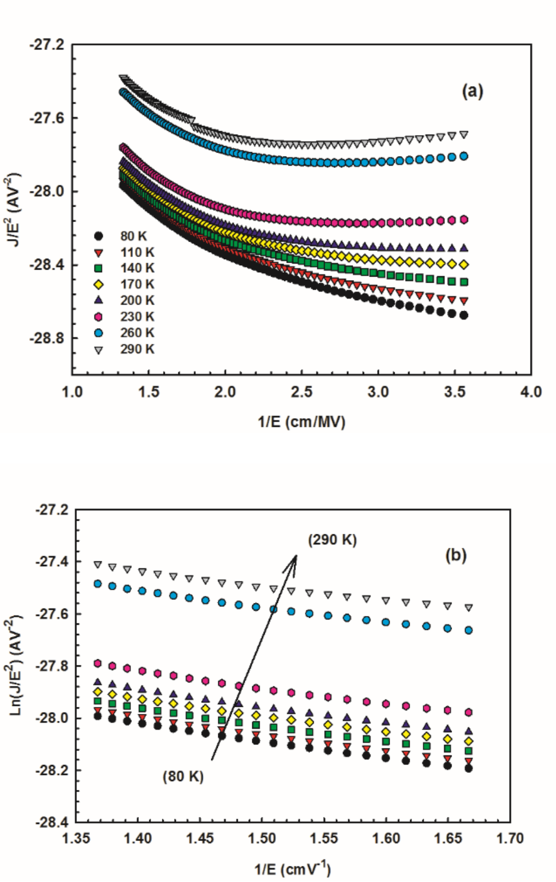

Figure 5*. (a) The temperature dependent and (b) the linear Fowler-Nordheim relation of reverse bias characteristics for (AuZn)/TiO₂/p-GaAs MIS structure*

Table 2. The calculated values of barrier height from the slope and R-squared values of the (AuZn)/TiO_2/p-GaAs MIS structure in the temperature range of 80-290 K.

Temperature (K)	Slope	Φ_B (eV)	R^2
80	0.668	0.317	0.998
110	0.653	0.312	0.997
140	0.638	0.308	0.996
170	0.63	0.305	0.997
200	0.628	0.304	0.995
230	0.628	0.304	0.993
260	0.595	0.294	0.993
290	0.547	0.278	0.990

Also, the R-squared values should be 1 to indicate the good agreement of the FN tunneling mechanism. As can be seen from the Table 2, the values R^2 are very close to 1 that supporting the FN tunneling in the given voltage and field region.

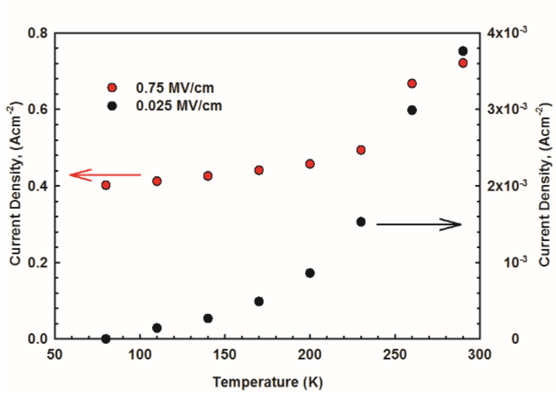

Figure 6*. The current density versus temperature plot for low and moderate field values for (AuZn)/TiO₂/p-GaAs MIS structure*

To better understand the field dependency of the conduction mechanism as function of temperature we have plotted the current density versus temperature plot for low and moderate field values and given in Fig. 6. As can be seen from the figure that while studying under low field (0.25 MV/cm) the temperature dependence of the leakage current is obvious for all temperatures from 80 to 290 K. The temperature dependence behavior of the leakage current reveals that the dominant mechanism is the Schottky emission under low field. But, there was almost no leakage current dependence on the temperature under 230 K in moderate field (0.75 MV/cm), whereas the current increases above 230 K with the increase of temperature. The temperature independent behavior of the leakage current at this point can be the evident of the FN tunneling under high field effect [30].

Space Charge Limited Current (SCLC)

The behavior of the reverse bias current were analyzed to determine the possibility of the space-charge-limited-current mechanism at moderate bias voltage at V=((-0.23)-(2.32))V.

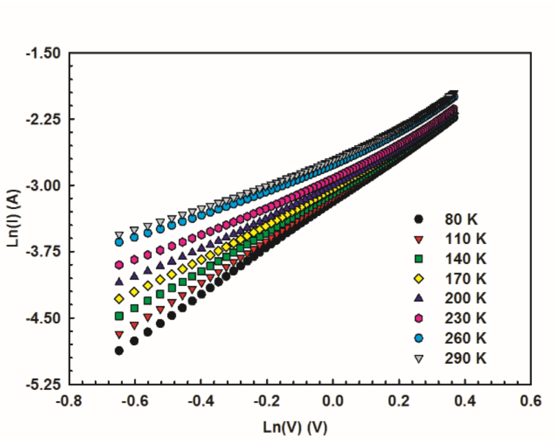

Figure 7. *The double logarithmic reverse-bias I-V plots of (AuZn)/TiO_2/p-GaAs MIS structure.*

Table 3. The calculated slope for each temperature and the R-squared values of the double logarithmic reverse-bias $I-V$ plots of (AuZn)/TiO_2/p-GaAs MIS structure

Temperature (K)	Slope	R^2
80	2.59	1.000
110	2.43	1.000
140	2.26	0.999
170	2.10	0.997
200	1.94	0.994
230	1.66	0.986
260	1.78	0.991
290	1.60	0.985

The double logarithmic reverse-bias $I-V$ plots in Fig. 7 show a linear behavior with a constant for all temperatures. The calculated values of slope for each temperature and the R-squared values are tabulated in Table 3. So, there is no relation between the current given as $I \propto V^{m+1}$ [34]. This means, the SCLC mechanism is not present for (AuZn)/TiO_2/p-GaAs MIS structures in the given reverse bias region.

Conclusion

In the recent study, we investigated the reverse bias current conduction mechanisms of (AuZn)/TiO_2/p-GaAs metal-insulator-semiconductor (MIS) structure in the temperature range of 80-290 K. The analysis of the reverse current underlines that the main process in leakage current flow is the carrier injection through a barrier at the material electrode interface. The temperature dependence behavior of the leakage current reveals that the dominant mechanism is the Schottky emission under low field. But, there was almost no leakage current dependence on the temperature at temperatures under 230 K in moderate field (0.75 MV/cm), whereas the current increases above 230 K with the increase of temperature. The temperature independent behavior of the leakage current at this point can be the evident of the FN tunneling under high field effect.

Acknowledgments

The author thanks to Prof. Dr. Ş. ALTINDAL and Prof. Dr. S. ÖZÇELİK for sample preparation and giving permission to use the experimental equipment.

References

[1] Y. Şafak-Asar, T. Asar, Ş. Altındal, S. Özçelik, J. Alloys Compd. 628 (2015) 442-449.
[2] Y. Şafak Asar, T. Asar, Ş. Altındal, S. Özçelik, Philos. Mag. A (In Press)
[3] C. H. Liu, T.K. Lin, S.J. Chang, Solid-State Electron. 49 (2005) 1077-1080.
[4] C. F. Yen, M.K. Lee, Solid-State Electron. 73 (2012) 56-59.
[5] S. Kim, D.-M. Geum, M.-S. Park, C.Z. Kim, W.J. Choi, Sol. Energy. Mat. Sol. C. 141 (2015) 372-376.
[6] X. Qian, M. Kawai, H. Goto, J. Li, Com. Mater. Sci. 108 (2015) 258-263.
[7] Y. Wang, X. Zhang, M. Guo, X. sun, Y. Yu, J. Xi, Opt. Laser Technol. 74 (2015) 43-47.
[8] S. Demirezen, E. Özavcı, Ş. Altındal, Mater.Sci. Semicond. Process 23 (2014) 1-6.
[9] E. Özavcı, S. Demirezen, U. Aydemir, Ş. Altındal, Sens. Actuators A 194 (2013) 259-268.
[10] O. Mitrofanov, M. Manfra, J. Appl. Phys. 95 (11) (2004) 6414-6419.
[11] R.T. Tung, J. Vac. Sci. Technol. B 11 (4) (1993) 1546-1552.
[12] E.H. Rhoderick, R.H. Williams, Metal-Semiconductor Contacts, second ed., Clarendon Press, Oxford, 1988.
[13] W. Yang, J. Marino, A. Monson, C.A. Wolden, Semicond. Sci. Technol. 21 (2006) 1573-1579.

[14] Q.-Z. Zhang, B. Zhu, L.-f. Zhang, S.-J. Ding, Microelectron. Eng. 122 (2014) 1-4.
[15] R.J.H. Clark, The Chemistry and titanium and Vanadium, An Introduction to the Chemistry of the Early Transition Elements, Elsevier, New York,1968 (p.70).
[16] S. Santangelo, G. Faggio, G. Messina, e. Fazio, F. Neri, Ge. Neri, Sens. Actuators B 178 (2013) 473-484.
[17] G. Impellizzeri, V. Scuderi, L. Romano, E. Napolitani, R. Sanz, R. Carles, V. Privitera, J. Appl. Phys. 117 (2015) 105308.
[18] P.R. Ohodnicki, C. Wang, S. Natesakhawat, J.P. Baltrus, T.D. Brown, J. Appl. Phys. 111 (2012) 064320.
[19] M.G. Manera, A. Colombelli, R. Rella, A. Caricato, P.D. Cozzoli, M. Martino, L. Vasanelli, J. Appl. Phys. 112 (2012) 053524(11 pp)
[20] S. Zen, Y. Inoue, R. Ono, J. Appl. Phys. 117 (2015) 103302 (5 pp).
[21] S.-K. Kim, C.V.V. Gopi, J.-C. Lee, H.-J. Kim, J. Appl. Phys. 117 (2015) 163104.
[22] K. Lv, M. Zhang, C. Liu, G. Liu, H. Li, S. Wen, Y. Chen, S. Ruan, J. alloys Compd. 580 (2013) 614-617.
[23] S. M. Sze, Physics of Semiconductor Devices, 2nd Ed. Willey, New York, 1981.
[24] E.H. Rhoderick and R.H. Williams, Metal-Semiconductor Contacts, 2nd Ed. Clarendon Press, Oxford, 1988.
[25] E.H. Nicollian and J.R. Brews, Metal Oxide Semiconductor (MOS) Physics and Technology, John Willey & Sons, New York, 1982.
[26] D. Tomer, S. Rajput, L.J. Hudy, C.H. Li and L. Li, Applied Physic Letter 106 (2015) 173510 (4 pp).
[27] A.A. Hussain, A.R. Pal, H. Bailun, J. Chutia, D.S. Patil, J. Phys. D: Appl. Phys. 46 (2013) 325301 (10 pp).
[28] P. Laha, A.B. Panda, S. Dahiwale, K. Date, K.R. Patil, P.K. Barhai and A.K. Das, Thin Solid Films 519 (2010) 1530-1535.
[29] S. Chakrabory, M.K. Bera, S. Bhattacharya, C.K. Maiti, Microelectronic engineering 81 (2005) 188-193.
[30] M. Sometani, D. Okamooto, S. Harada, H. Ishimori, s. Takasu, T. Hatakeyama, M. Takei, Y. Yonezawa K. Fukuda, H. Okumura, J. Appl. Phys. 117 (2015) 024505 (6 pp).
[31] J. Kim, S.A. Krishnan, S. Narayanan, M.P. Chudzik, M.V. Fischetti, Microelectronics Reliabilitiy 52 (2012) 2907-2913.
[32] M. Chandra Sekhar, P. Kondaiah, s.V. Jagadeesh Chnadra, G. Mohan Pao, S. Uthanna, Surf. Interface Anal. 44 (2012) 1299-1304.
[33] W. Yang, J. Marino, A. Monson and C.A. Wolden, Semicond. Sci. Technol. 21 (2006) 1573-1579.
[34] Ö. Vural, Y. Şafak, Ş. Altındal A. Türüt, Current Applied Phys. 10 (2010) 761-765.
[35] S.B.K. Aydın, D.E. Yıldız, H. Kanbur Çavuş, R. Şahingöz, Bull. Mater. Sci. 37 (2014) 1563-1568.2003.